Plant and Soil 94, 59–85 (1986). Ms. 6406

Penetration of soil aggregates of finite size

II. Plant roots

R. K. MISRA, A. R. DEXTER and A. M. ALSTON
Department of Soil Science, Waite Agricultural Research Institute, The University of Adelaide, Glen Osmond, South Australia, 5064

Received 15 May 1985. Revised October 1985

Key words Cohesion *Gossypium hirsutum* *Helianthus annuus* Penetrometer resistance *Pisum sativum* Plastic failure Radial stress Root diameter Root growth pressure Soil aggregates Tangential stress Tensile stress

Summary The axial force required for penetration of soil aggregates by roots of pea (*Pisum sativum* cv. Greenfeast), cotton (*Gossypium hirsutum* cv. Sicot 3) and sunflower (*Helianthus annuus* cv. Hysun) seedlings was measured. Effects of aggregate size and strength on root penetration behaviour were investigated. Maximum axial root growth pressure (P_r) was estimated from the maximum axial root growth force (F_{max}) and mean root diameter.

F_{max}, time (T_{max}) to attain F_{max}, and P_r all increased with increase in size and strength of aggregates. A significant interactive effect of size and strength of aggregate on root diameter was observed. F_{max}, T_{max} and root diameter were significantly different for different plant species.

Maximum penetrometer pressure (P') was compared with the axial pressures generated during root penetration. The penetrometer probe was found to overestimate the root growth pressure by a factor of 1.8 to 3.8. P_r/P' decreased with increase in size and strength of aggregates.

A theory was developed to estimate radial and tangential stresses adjacent to the soil-root interface assuming cylindrical deformation by the root in aggregates of finite size. The stresses were calculated using shear cohesion values, estimated from tensile strength measurements, and with an assumed value of soil internal friction. Radial and tangential stresses adjacent to the root axis increased with increase in dimensionless aggregate radius and aggregate strength. Tensile stress adjacent to the root axis is predicted to result in plastic failure of finite sized aggregates during root penetration.

Introduction

Soil mechanical resistance affects the penetration and growth of plant roots in all soils, not just in those of high strength. Although quantitative information on soil resistance to root penetration is essential for an understanding of the behaviour of roots, there are few experiments in which root penetration forces have been directly measured[11,28,40].

In the past, the penetrating ability of plant roots has been assessed from the resistance to blunt and sharp penetrometer probes[6,7,20,21,27,30,32,36]. However, soil resistance to probe penetration is much greater than the resistance to plant roots[11,28,41] although the relative

responses of probes and roots to soil impedance are strikingly similar. One argument frequently appearing in the literature about the differential responses of probes and plant roots relates to the flexible nature of the roots, by virtue of which they are able to take advantage of planes of weakness in the soil. In contrast, metal probes, being rigid, must follow a straight path. The abilities of roots of different plant species to penetrate a given soil could be very different[16], and in a macroscopically structured soil this may depend on the elastic properties of roots[37]. Direct measurements on root buckling[39], deflection[8,19,29] and root penetration into soil having cracks of known width[38] have shown that roots of different plant species may differ in their ability to take advantage of the planes of weakness.

It has been documented earlier that soil may be deformed differently by probes and roots. Blunt penetrometer probes (total tip angle = 60°) deform the soil almost spherically[10,13,25] whereas plant roots and sharp probes (total tip angle = 10°) deform the soil almost cylindrically[5,20]. The theory of expansion of cylindrical cavities under internal, uniform pressure has been successfully applied to explain soil deformation by root tips[20]. This is similar, in principle, to the spherical deformation around blunt probes[13,25,35], in which plastic failure of soil occurs out to some distance from the centre of the cavity.

Although the root penetration force in soil is rarely measured, some data on the maximum pressures which roots can exert in the axial direction are available. They range from 610 kPa to 1300 kPa[12,14,26,28,31]

Most studies on root penetration have been done either with homogeneous, remoulded soil compacted to a known density[30,36] or with confined, homogeneous granular media (*e.g.* glass beads) under an applied stress[1,2,3,15,17,34]. Use of macroscopically structured soil has largely been avoided firstly because the statistical concept of stress and strain can not be employed and secondly because the mechanical properties of bulk soil have little relevance to the resistance met by the root tip in these soils[19]. A theory has yet to be developed to describe the radial and axial stress to the plant root in macroscopically structured soil.

This paper describes the variation in axial root growth pressures of pea, cotton and sunflower during root penetration into aggregates of different sizes and strengths. A theoretical estimate of radial and tangential stress adjacent to the root is given.

Theory of root penetration into soil aggregates

The penetration of a plant root into a soil aggregate presents a

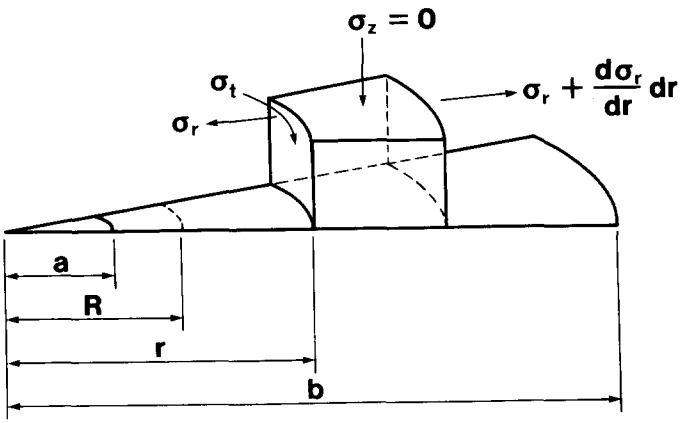

Fig. 1. Schematic illustration of soil aggregate of radius b, penetrated by a plant root of radius a. R is the radius of the plastic front. σ_r and σ_t are the radial and tangential stresses, respectively at a radial distance, r, from the centre of the circular aggregate face. Normal stress, σ_z in the z-direction, is assumed to be zero.

problem similar to that encountered with the expansion of a tube under an internal, uniform pressure[10]. To simplify the problem, the following assumptions are made.

1. Soil aggregates are composed of incompressible, frictional, elastic-plastic material, and due to lack of confinement around the aggregate, root volume is accommodated by the expansion of the aggregate boundary.

2. The stress distribution around the root is axially symmetric. This assumes that the soil aggregates are cylindrical.

3. The soil aggregates exhibit elasticity at pressures lower than an ultimate state of stress at which the aggregate fails plastically[25,35].

4. Compressive stresses are positive and tensile stresses are negative.

5. The pressure, P, in directions radial to the root axis is equal to the axial root growth pressure.

Figure 1 shows a cross-section of an aggregate (or radius b) and a root (of radius a) penetrating the centre of the aggregate at a uniform pressure P. The radial distance from the centre point of the circular cross section is r and the radial distance to the plastic front is R. The radial normal stress on a volume element shown in Fig. 1 is represented by σ_r and the stress in the direction normal to it is the tangential stress σ_t.

The general expression for the radial normal stress in an elastic, cylindrical tube (p 58, Timoshenko and Goodier[33]) is

$$\sigma_r = (A/r^2) + B. \tag{1}$$

where A and B are constants, and have real values which depend on the stress boundary conditions at a and b. Because there is no external force on the aggregate, the boundary conditions are

$$\text{at } r = a: \quad (A/a^2) + B = P \tag{2}$$

$$\text{and at } r = b: \quad (A/b^2) + B = 0. \tag{3}$$

Eqns 2 and 3 may be solved for constants A and B, which are

$$A = \frac{Pa^2 b^2}{b^2 - a^2} \quad \text{and} \quad B = \frac{-Pa^2}{b^2 - a^2}. \tag{4}$$

These values of A and B can be substituted in Eqn 1 to give

$$\sigma_r = \frac{P[(b^2/r^2) - 1]}{(b^2/a^2) - 1}. \tag{5}$$

The expression for the tangential stress can be obtained by applying the equilibrium equation of stresses on any volume element as shown in Fig. 1. This equation is

$$\frac{d\sigma_r}{dr} + \frac{1}{r}(\sigma_r - \sigma_t) = 0. \tag{6}$$

Combining Eqns 5 and 6 gives

$$\sigma_t = \frac{-P[(b^2/r^2) + 1]}{(b^2/a^2) - 1}. \tag{7}$$

Inspecting Eqns 5 and 7, we find σ_r takes the value of zero and P at $r = b$ and $r = a$, respectively; whereas σ_t is always less than P and negative. The principal stresses (σ_I = major, σ_{II} = intermediate and σ_{III} = minor) can be assigned as follows.

$$\sigma_I = \sigma_r \quad \text{and} \quad \sigma_{II} = \sigma_{III} = \sigma_t. \tag{8}$$

Maximum shear stress (τ_{max}) is given by

$$\tau_{max} = \frac{\sigma_I - \sigma_{III}}{2} = \frac{\sigma_r - \sigma_t}{2}. \tag{9}$$

and the shear strength or stress (τ) at soil failure is

$$\tau = c + \sigma_n \tan \phi. \tag{10}$$

The stresses σ_r and σ_t are found to be related to cohesion (c) and the angle of internal friction (ϕ). The normal stress (σ_n) acting on the shear planes[23] is related to σ_r and σ_t as follows.

$$\sigma_n = \sigma_r \cos^2 \theta + \sigma_t \sin^2 \theta, \tag{11}$$

where $\theta = (\pi/4 + \phi/2)$.

Cohesion and the angle of internal friction for any soil can be determined from triaxial shear tests. However, the effect of ϕ on σ_r and σ_t for a blunt probe has been found to be much smaller than the effect of c[25]. In unsaturated soils, ϕ varies from 25° to 45°, and is typically 35°. Values of c can be estimated from unconfined compression tests[24] if ϕ is known or assumed.

Eqns 10 and 11 may be rearranged to give

$$\sigma_t = \left(\frac{1 - \sin\phi}{1 + \sin\phi}\right) \sigma_r - \frac{2c\cos\phi}{1 + \sin\phi}. \tag{12}$$

A solution of Eqn 6 which satisfies the stress relation of Eqn 12 in the plastic zone $r < R$ may be written[20] as

$$\sigma_r = A'(1 + \sin\phi)(R/r)^{2\sin\phi/(1+\sin\phi)} - c\cot\phi \tag{13}$$

$$\sigma_t = A'(1 - \sin\phi)(R/r)^{2\sin\phi/(1+\sin\phi)} - c\cot\phi. \tag{14}$$

In Eqns 13 and 14, A' is a constant which can be estimated from the assumption of continuity of stresses at the plastic-elastic interface, $r = R$.

$$\left(\frac{\sigma_r}{\sigma_t}\right)_{\text{elastic}} = \left(\frac{\sigma_r}{\sigma_t}\right)_{\text{plastic}} \tag{15}$$

or,

$$\frac{(b^2/R^2) - 1}{-[(b^2/R^2) + 1]} = \frac{A'(1 + \sin\phi) - c\cot\phi}{A'(1 - \sin\phi) - c\cot\phi} = \frac{X}{Y}, \tag{16}$$

from which

$$A' = \frac{c\cot\phi\,(X - Y)}{(1 - \sin\phi)X - (1 + \sin\phi)Y} \tag{17}$$

Now we know that when P is raised to an ultimate pressure P_r, $\sigma_r = P_r$ at $r = a$ and the aggregate fails plastically. On substitution of σ_r by P_r and r by a, Eqn 13 becomes

$$\frac{P_r + c\cot\phi}{A'(1 + \sin\phi)} = (R/a)^{2\sin\phi/(1+\sin\phi)} \tag{18}$$

or,

$$\log R = \left(\frac{1 + \sin\phi}{2\sin\phi}\right) \log \frac{P_r + c\cot\phi}{A'(1 + \sin\phi)} + \log a. \tag{19}$$

Eqn 19 is transcendental in R; hence, it can be solved iteratively to obtain estimates of R for plant roots of different radii penetrating aggregates of various radii. In Eqn 19, P_r is the maximum axial root growth pressure. It should be noted that for sandy soils, whose $c \sim 0$,

the values of R would be meaningless in practice because aggregation in such soils does not occur. However, for cohesive soil material like saturated clay, which has very little internal friction ($\phi \sim 0$), Eqn 12 reduces to

$$\sigma_r - \sigma_t = 2c. \tag{20}$$

From Eqns 6 and 20

$$\frac{d\sigma_r}{dr} + \frac{2c}{r} = 0. \tag{21}$$

Eqn 21 is solved to obtain

$$\sigma_r = -2c \log r + B' \tag{22}$$

From Eqns 20 and 22,

$$\sigma_t = -2c \log r - 2c + B'. \tag{23}$$

Applying the assumption of continuity of stresses at the plastic-elastic interface, $r = R$ (*i.e.* Eqn 14), we obtain

$$\frac{(b^2/R^2) - 1}{-[(b^2/R^2) + 1]} = \frac{-2c \log R + B'}{-2c \log R - 2c + B'} = \frac{X'}{Y'}. \tag{24}$$

from which

$$B' = \frac{2c(X' - Y') \log R + 2cX'}{X' - Y'}. \tag{25}$$

At the time of aggregate failure, $\sigma_r = P_r$ at $r = a$. Under this condition, Eqns 22 and 25 are combined to give

$$P_r = -2c \log a + \frac{2c(X' - Y') \log R + 2cX'}{X' - Y'}. \tag{26}$$

or,
$$\log R = \frac{(X' - Y')(P_r + 2c \log a) - 2cX'}{2c(X' - Y')} \tag{27}$$

Eqn 27 is transcendental in R and must be solved iteratively to obtain estimates of R.

Materials and methods

The soil used in this experiment was a loam from the top 100 mm layer of a red-brown earth (rhodoxeralf) at Mintaro, South Australia. The soil had 2.1% coarse sand, 38.5% fine sand, 34.7% silt and 20.8% clay. The organic matter content of this soil was 4.3% and the Casagrande plastic limit was 25.6%.

Laboratory preparation of soil aggregates

Aggregates collected from the field were unsuitable for this study due to their large variabilities in density and strength. Hence artificial aggregates were prepared in the laboratory from sieved (< 2 mm) air-dry soil. Six different size ranges of aggregates (4.0–6.7, 6.7–9.5, 9.5–12.7, 12.7–19.0, 19.0–22.0, 22.0–29.0 mm) were prepared and the strength of each size range of aggregates was varied to 3 levels (referred to as S_1, S_2 and S_3 in the text) by adding different quantities of poly(vinyl alcohol) (PVA) during their preparation. The method of aggregate preparation was essentially same as reported previously by Misra *et al.*[25]. The first batch of aggregates (S_1) had no added PVA and was prepared by spraying deionised water on to sieved, air-dry soil until the soil reached saturation. The saturated soil was left at 20°C in a sealed container overnight before being dried at 60°C for 48 h. The dried soil was broken by hand, the edges of the aggregates were rounded-off and finally sieved to provide the six different size ranges as listed above. The two other batches of aggregates (S_2 and S_3) were prepared by adding 100 ml of 0.02% and 0.20% PVA solution, respectively to 1 kg (oven-dry) lots of soil before water was added to bring the soil to saturation. The rest of the aggregate-preparation procedure was similar to that described for S_1. All batches of aggregates were treated with nutrient solution I (consisting of 13.49 g $Ca(NO_3)_2 . 4H_2O$, 12.58 g $NaH_2PO_4 . 2H_2O$, 6.48 g KNO_3, 7.70 g $MgSO_4 . 7H_2O$ in 2L) which was added at 10 ml kg^{-1} oven-dry soil prior to saturating the soil during aggregate preparation.

Method of growing plants for root penetration studies

Seeds of cotton (*Gossypium hirsutum* cv. Sicot 3) and sunflower (*Helianthus annuus* cv. Hysun) were planted in 'Dispo' growth bags (160 mm long and 140 mm wide) containing 20 ml of 10% strength of nutrient solution II. Full strength nutrient solution II contained 6 m*M* KNO_3, 4 m*M* $Ca(NO_3)_2 . 4H_2O$, 2 m*M* $NH_4H_2PO_4$, 1 m*M* $MgSO_4 . 7H_2O$ per litre and trace elements at concentrations reported by Johnson *et al.*[22]. Pea (*Pisum sativum* cv. Greenfeast) seeds were soaked overnight prior to planting in vermiculite. The vermiculite had been saturated with 10% strength of nutrient solution II and allowed to drain for 24 h. All seedlings were grown at 20°C under a bank of fluorescent tube lights (90 μmol m^{-2} sec^{-1}) and the roots were shielded from light. Seedlings grown in 'Dispo'bags were watered daily to make up for the evaporation losses. After 3 days, the seedlings were transferred to the apparatus shown in Fig. 2.

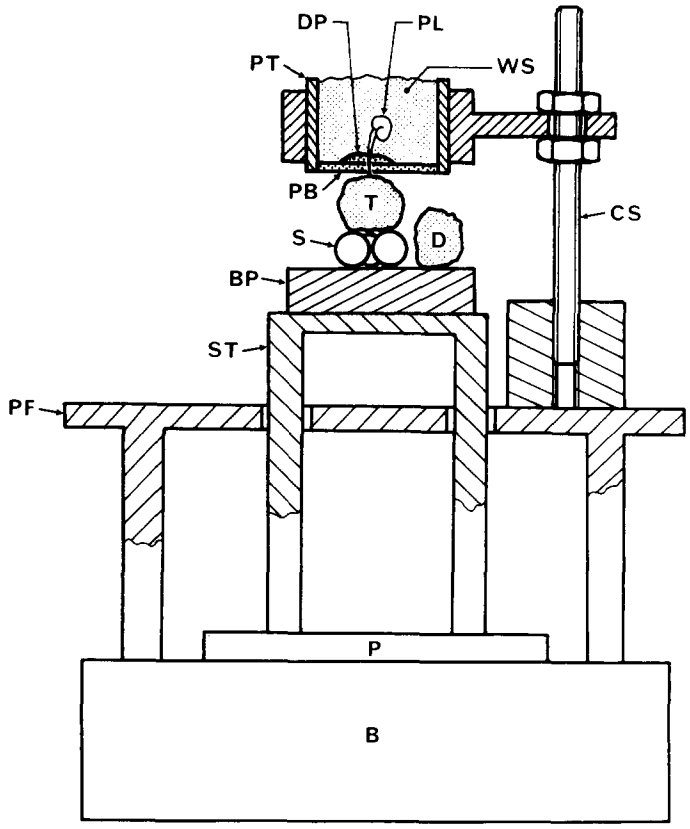

Fig. 2. Side view of the apparatus for measuring axial root growth force. The main root axis of a plant (PL) is anchored to the plaster base (PB) of the plastic tube (PT) by dental plaster (DP). The tube PT with 0.5 mm of the root protruding from PB is held by the clamp stand (CS) so that the root tip touches the test aggregate (T). The aggregate is supported by 3 wet porous spheres (S), glued together. T rests on a stand (ST) connected to pan (P) of a digital electronic balance (B). BP, a wet plaster block between ST and S is an additional water reservoir to reduce water loss from T. More details are given in the text.

Measurement of axial root growth force

Axial root growth force of pea, cotton and sunflower was measured on aggregates of six different sizes and three different strengths (S_1, S_2 and S_3) using 3-day-old seedlings. On any single occasion, radicles of 3 plants (one each of pea, cotton and sunflower) were allowed to penetrate 3 separate aggregates randomly chosen from one of the 18 possible combinations of size and strength. Each plant, aggregate size and strength were replicated six times so that 324 measurements of axial root growth force were obtained.

All aggregates used for measurement of axial root growth force

were slowly wetted from air dry to saturation on sintered funnels over 48 h and were then drained to a water potential of -2 kPa in the 48 h following saturation. An hour before the aggregate was set up for root penetration, penetrometer pressure was measured on 2 replicate aggregates of the kind chosen for root penetration. Penetrometer pressures were measured as reported previously[25]. A 1 mm diameter probe (total cone angle = 60°) was motor driven at 3 mm min^{-1} into the aggregate, supported by 3 glass spheres and the maximum penetration force was measured with a digital eletronic balance. There were 12 replicate measurements of penetrometer pressure representing each size and strength of aggregate.

The apparatus for measuring the axial root growth force (Fig. 2) consisted of 2 parts: the first part held the root protruding from a plastic tube (PT) in position on the top of the aggregate and the other part was a digital electronic balance (B) which indicated axial root growth force. Three plants and three balances were always in use. The axial root growth forces on the balances were recorded at 10 minutes intervals by a microcomputer (not shown in the figure) and subsequently printed.

The electronic balance (B) measured the force with a resolution of 0.0001 N and the pan deflection was negligible. A plastic platform (PF) standing outside the pan (P) held the clamp stand (CS) and also permitted ventilation over the pan thus removing heat generated by the balance. The plastic stand (ST) resting on the pan (P) supported the test aggregate (T) during the measurements of axial root growth force. The test aggregate (T) was supported on 3 porous spheres (S, each 15 mm diameter), glued together and the aggregate and the spheres all were brought to a water potential of -2 kPa as described in the preceding paragraphs. An additional block of plaster (BP) wetted to a water potential of -2 kPa was provided beneath the porous spheres to minimize water loss from the aggregate T. A duplicate aggregate (D) of the same treatment as T, was kept on the plaster block to measure water loss from the aggregate during the experiment.

Each 3-day old seedling (PL) was planted in soil held in a plastic tube (PT), 45 mm diameter, 50 mm long which had a 1 mm thick plaster base (PB). The root tip protruded about 0.5 mm outside the tube through a hole made on the plaster base prior to planting. The root was anchored to the plaster base by a drop of liquid dental plaster (DP). The rest of the root system in the tube was supplied with wet soil, WS (water content 25% by wt) to which nutrient solution I had been added at the same rate as that for the aggregates. To prevent desiccation of the root during the experiment, the plaster base PB

was wetted by spraying with water. On no occasion did wetting the base affect anchorage of the roots. The plastic tube with the root protruding from the plaster base was then held aligned to the aggregate by the clamp stand (CS). The air gap between PB and T never exceeded 0.5 mm. The plants and aggregates were kept covered by a polythene sheet attached to PF. Several water-filled pots kept on PF maintained a humid environment under the polythene sheet. For clarity, the polythene sheet and water filled pots are not shown in Fig. 2.

The root penetration experiment took 20–24 h for each set of three plant seedlings. The axial root growth force reached a maximum in about 15–20 h for most of the aggregates and it dropped slowly thereafter. The roots either penetrated into the aggregate or were deflected and grew in the air gap. Shortly after the axial root growth force reached the maximum, the plant roots with aggregates intact were removed from the apparatus. The diameter of the root was measured at the air gap and at 1 mm behind the root tip by a travelling microscope with an accuracy of 10^{-2} mm. The water loss from the duplicate aggregate (D) was negligible compared with the values of F_{max}. Therefore, F values were obtained directly from the balance readings which did not have to be corrected for changes in aggregate weight.

The maximum axial root growth pressure (P_r) was estimated using the maximum axial root growth force (F_{max}) and root diameter (d_r) as

$$P_r = \frac{4F_{max}}{\pi d_r^2}, \tag{28}$$

where d_r is the mean of the root diameters at the air gap and 1 mm behind the root tip.

Determination of shear cohesion (c)

Aggregates of 6 size ranges and 3 strengths prepared as for the root penetration experiment were slowly wetted over 48 h at 20°C from the air-dry state to saturation on porous ceramic plates, which were covered with plastic lids to prevent evaporation. The aggregates were drained on the same plates to a water potential of -2 kPa over the next 48 h. The tensile strength of 20 replicate aggregates for each size and strength was measured in an indirect tension test by crushing them between 2 flat, parallel plates, using a loading frame and a top-loading balance. The tensile strength (T') was calculated from the force at failure (F) following Dexter and Kroesbergen[9] as shown below.

$$T' = 0.576\, F/d^2 \tag{29}$$

where d is the aggregate diameter *i.e.* mean of the mesh sizes of the two sieves used to separate the aggregate. Shear cohesion, c, was estimated from the tensile strength using the relationship

$$c = T'/0.48 \tag{30}$$

suggested by Koolen and Vaandrager[24].

These estimated values of c were averaged over the six aggregate sizes for each of the aggregate strengths (S_1, S_2 and S_3) used in the root penetration experiment.

Results

The measured and estimated parameters involving root penetratrion into aggregates of different sizes and strengths were subjected to analysis of variance (Table 1).

The maximum axial root growth force (F_{max}), and the time (T_{max}) taken for the development of maximum axial root growth force, and the maximum penetrometer pressure (P') were significantly affected by the differences in aggregate size and strength. Maximum axial root growth pressures (P_r) estimated from F_{max} and the mean root diameters (d_r) were also affected significantly by the size and strength of aggregates, but no differences between the plants were detected. All other measured parameters relating to P_r were significantly different for different plants. Root diameters measured at the air gap and near the tip were only slightly affected by aggregate size and strength.

The proportion of roots penetrating into the aggregates and the proportion which were deflected from the aggregate surface were not calculated because there were only six replicates. Information on root deflection already exists[8,19]. In our experiment, all measured parameters had some missing values and although this did not affect the analysis of variance, a single LSD value cannot be given due to different numbers of missing values in different treatments.

Axial root growth force

The maximum axial root growth forces (F_{max}) required by all 3 plant species to penetrate aggregate of various sizes are presented in Fig. 3. The effect of aggregate size on F_{max} was much larger than the effect of aggregate strength. Therefore, the F_{max} values in Fig. 3 have been averaged across the three strengths. For all plant species, increasing aggregate diameter (d) beyond 20 mm did not increase F_{max} significantly. It is clear that increased aggregate size increased impedance to root penetration. For the three plants used in the experiment, the effect of aggregate diameters over the range $5 < d <$ 26 mm can be described

Table 1. Results of analysis of variance tests for the parameters involved in the root penetration experiment

Treatments in the experiment	Maximum axial root growth froce (F_{max})	Maximum time taken to reach F_{max} (T_{max})	Root tip diameter (RTD)	Root diameter in the air gap (RDA)	Mean root diameter (d_r)	Maximum penetrometer pressure (P')	Maximum root growth pressure (P_r)
Aggregate strength (PVA content)	**	**	NS	NS	NS	**	**
Aggregate size	**	**	*	NS	*	**	**
Aggregate strength x aggregate size	NS	NS	*	*	**	NS	NS
Plant species	**	**	**	**	*	NA	NS
Aggregate strength x plant species	**	NS	NS	NS	NS	NA	NS
Aggregate size x plant species	NS	NS	NS	NS	NS	NA	NS
Aggregate strength x aggregate size x plant species	NS	NS	NS	NS	NS	NA	NS

** indicates significance at $P \leqq 0.01$
* indicates significance at $P \leqq 0.05$
NS indicates not significant at $P \leqq 0.05$
NA indicates not applicable

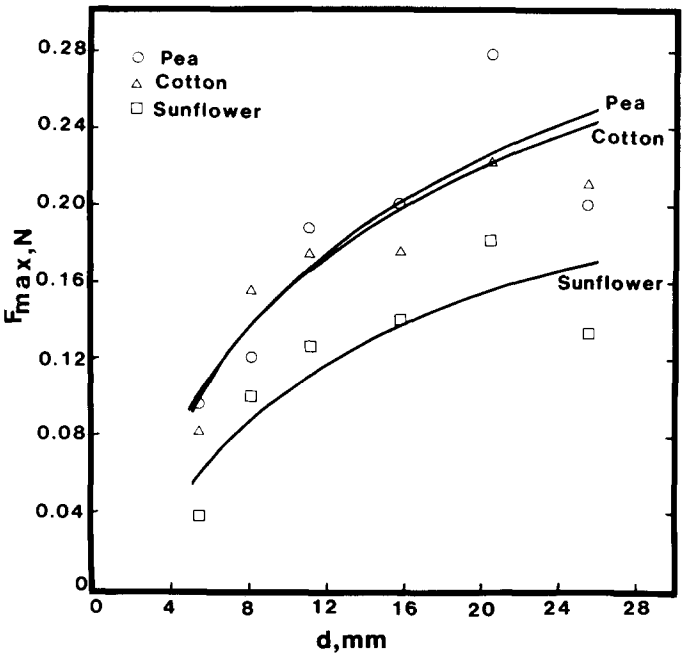

Fig. 3. Maximum axial root growth force (F_{max}) of pea, cotton and sunflower as a function of aggregate diameter (d).

for pea by $F_{max} = 0.095 \ln d$ ($R^2 = 0.73$), (31)

for cotton by $F_{max} = 0.091 \ln d$ ($R^2 = 0.68$) and (32)

for sunflower by $F_{max} = 0.071 \ln d$ ($R^2 = 0.74$) (33)

where F_{max} and d are expressed in N and mm, respectively. Over the whole size range of aggregates, F_{max} increased 3–4 fold from the smallest recorded value of 0.04 N.

For F_{max} there was a significant interaction between the plant type and aggregate strength (Table 2). Increasing the PVA content of the aggregates was expected to increase aggregate strength and for most plants, F_{max} did increase with increased PVA content.

Time taken for development of maximum axial root growth force

The time (T_{max}) taken for the development of maximum axial force F_{max} is shown in Fig. 4 as a function of aggregate diameter. All plant species took longer times to penetrate larger aggregates than smaller aggregates. The effect of aggregate diameter (d, mm) on T_{max} (min) can be described by

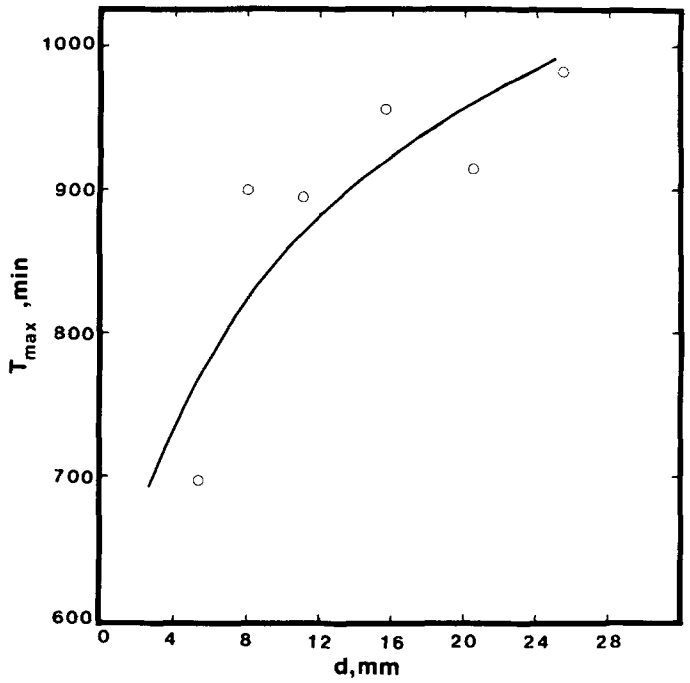

Fig. 4. Time taken (T_{max}) for the development of maximum axial root growth force as a function of aggregate diameter (d).

Table 2. Effect of aggregate strength and plant species on maximum axial root growth force (F_{max}) averaged over the sizes of aggregates*

	F_{max} (N)		
Aggregate strength (PVA content)	Pea	Cotton	Sunflower
S_1 (no PVA)	0.143b	0.165b	0.102a
S_2 (0.02% PVA)	0.198c	0.145b	0.110a
S_3 (0.20% PVA)	0.201c	0.200c	0.150b

* Figures in the table followed by same letter are not significantly different at $P \leqq 0.05$.

Table 3. Maximum time (T_{max}) taken for the development of maximum axial root growth force as a function of plant species and aggregate strength*

Plant species	T_{max} (min)	Aggregate strength (PVA content)	T_{max} (min)
Pea	980a	S_1 (no PVA)	850d
Cotton	1022b	S_2 (0.02% PVA)	842d
Sunflower	670c	S_3 (0.20% PVA)	980e

* Figures in each column followed by same letter are not significantly different at $P \leqq 0.05$.

$$T_{max} = 520 + 146 \ln d \qquad (R^2 = 0.73) \tag{34}$$

For different plants, T_{max} ranged from 670 min (11 h) for sunflower to 1022 min (17 h) for cotton (Table 3). Aggregate strength had a smaller effect on T_{max} than did the type of plant used in the experiment.

Root diameter

A comparison of root diameter near the tip (RDT) and root diameter in the air-gap (RDA) for different plants (Table 4) showed that the diameters were in the order pea > cotton > sunflower. For all plants, roots were more than twice as thick in the air gap than 1 mm behind the tip. The effects of the treatments on root diameters were not consistent, although the interactions between aggregate size and strength on RDT and RDA were statistically significant (Tables 5 and 6).

Axial root growth pressure

The effect of different aggregate sizes and strengths on the maximum axial root growth pressure (P_r) is shown in Table 7. Increase in aggregate strength and in aggregate diameter up to 22 mm increased P_r. All plant species had comparable P_r for the sizes and strengths of aggregates used in this study. In Fig. 5, P_r as a function of dimensionless aggregate radius b/a is shown for the three plants where b and a are the radii of the aggregate and the root respectively. The relationship of P_r and b/a for all plants can be represented by the fitted line shown in Fig. 5:

$$P_r = 0.092 \ln (b/a) \qquad (R^2 = 0.62). \tag{35}$$

Shear cohesion and penetrometer pressure

Shear cohesion (c) estimated from indirect tension tests, was 9 kPa for S_1 and S_2 aggregates and 14 kPa for S_3 aggregates. It appears that addition of 0.02% PVA solution to S_2 aggregates did not increase soil strength significantly. Maximum penetrometer pressure (P') is shown as a function of dimensionless aggregate radius (b/a') in Fig. 6 where a' represents probe radius.

For all the 3 strengths (S_1, S_2 and S_3), P' increased with increase in dimensionless aggregate radius b/a'. The relationship between P' (MPa) and b/a' is described within the experimental error

for S_1 by $P' = -0.174 + 0.267 \ln (b/a') \quad (R^2 = 0.94),$ (36)

for S_2 by $P' = -0.252 + 0.313 \ln (b/a') \quad (R^2 = 0.92),$ and (37)

for S_3 by $P' = -0.385 + 0.477 \ln (b/a') \quad (R^2 = 0.95).$ (38)

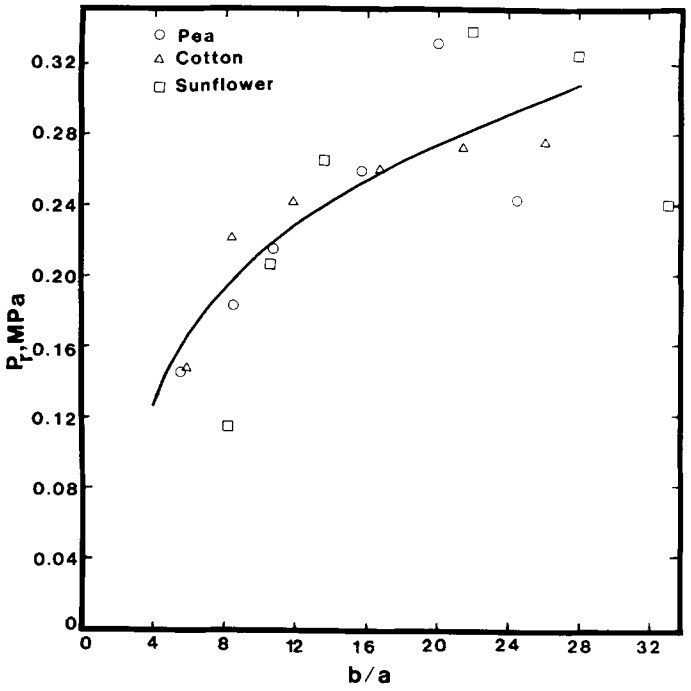

Fig. 5. Maximum axial root growth pressure (P_r) as a function of the dimensionless aggregate radius (b/a).

Table 4. Root diameter behind the tip (RDT) and in the air gap (RDA) for different plant species*

Plant species	RDT (mm)	RDA (mm)
Pea	0.60c	1.40e
Cotton	0.53b	1.36e
Sunflower	0.44a	1.04d

* Figures in each column followed by same letter are not significantly different at $P \leqq 0.05$.

Table 5. Root diameter (RDT) measured 1 mm behind the root tip as a function of size and strength of aggregate*

Aggregate strength (PVA content)	RDT (mm) for the aggregate size range (mm) of					
	4.0–6.7	6.7–9.5	9.5–12.7	12.7–19.0	19.0–22.0	22.0–29.0
S_1 (no PVA)	0.50ab	0.48a	0.49ab	0.49ab	0.57cd	0.54abcd
S_2 (0.02% PVA)	0.49ab	0.49ab	0.60d	0.54abcd	0.54abcd	0.54abcd
S_3 (0.20% PVA)	0.51abc	0.55bcd	0.50ab	0.50ab	0.53abc	0.57cd

* Figures in the table followed by same letter(s) are not significantly different at $P \leqq 0.05$.

Table 6. Root diameter (RDA) measured at the air gap as a function of size and strength of aggregate*

Aggregate strength (PVA content)	RDA (mm) for the aggregate size range (mm) of					
	4.0–6.7	6.7–9.5	9.5–12.7	12.7–19.0	19.0–22.0	22.0–29.0
S_1 (no PVA)	1.20ab	1.18ab	1.40cd	1.19ab	1.26abc	1.32bcd
S_2 (0.02% PVA)	1.21ab	1.21ab	1.42cd	1.18ab	1.24abc	1.32bcd
S_3 (0.20% PVA)	1.13a	1.46d	1.15ab	1.32bcd	1.28abcd	1.29abcd

* Figures in the table followed by same letter(s) are not significantly different at $P \leqq 0.05$.

Table 7. Maximum axial root growth pressure (P_r) as a function of size and strength of aggregate*

Aggregate size (mm)	P_r (MPa)	Aggregate strength (PVA content)	P_r (MPa)
4.0–6.7	0.136a	S_1 (no PVA)	0.218e
6.7–9.5	0.204b	S_2 (0.02% PVA)	0.233e
9.5–12.7	0.241b	S_3 (0.20% PVA)	0.263f
12.7–19.0	0.286cd		
19.0–22.0	0.310d		
22.0–29.0	0.252bc		

* Figures in each column followed by same letter(s) are not significantly different at $P \leqq 0.05$.

Radial and tangential stresses adjacent to the root

Estimation of the stresses adjacent to the root axis involves calculation of the radius of the plastic front (R) using Eqn 19. Our attempt to calculate R (such that $R < b$) was unsuccessful for the size range of aggregates used in this experiment. Fig. 7 shows a plot of R against root radius (a). To find a value of R less than b for the thinnest root of radius 0.4 mm, the aggregate radius must be greater than 54 and 24 mm for $c = 9$ and $c = 14$ kPa respectively. The smaller the root radius, the lower was the radius of aggregate (b) required to produce an R value smaller than b.

All aggregates used in this study had radii less than 15 mm, and the radial pressure (P_r) was assumed equal to the maximum axial pressure. Such aggregates under these conditions are undergoing plastic failure with the plastic zone spread up to b, for root radii between 0.4 and 1.0 mm. Hence, Eqn 15 is no longer valid. Now, R can be replaced by the maximum possible radius of the plastic zone in Eqns 13 and 14, which gives

$$\sigma_r = D(1 + \sin\phi)(b/r)^{2\sin\phi/(1+\sin\phi)} - c\cot\phi \quad (39)$$

and

$$\sigma_t = D(1 - \sin\phi)(b/r)^{2\sin\phi/(1+\sin\phi)} - c\cot\phi \quad (40)$$

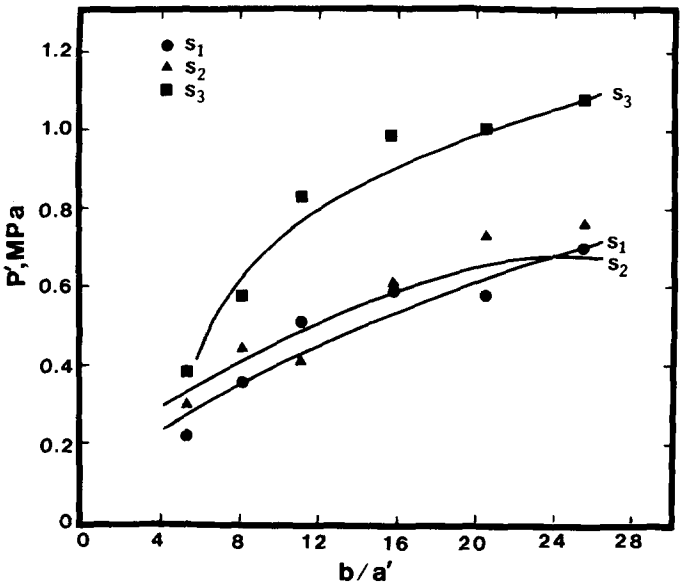

Fig. 6. Maximum penetrometer pressure (P') as a function of dimensionless aggregate radius (b/a') for S_1, S_2, and S_3.

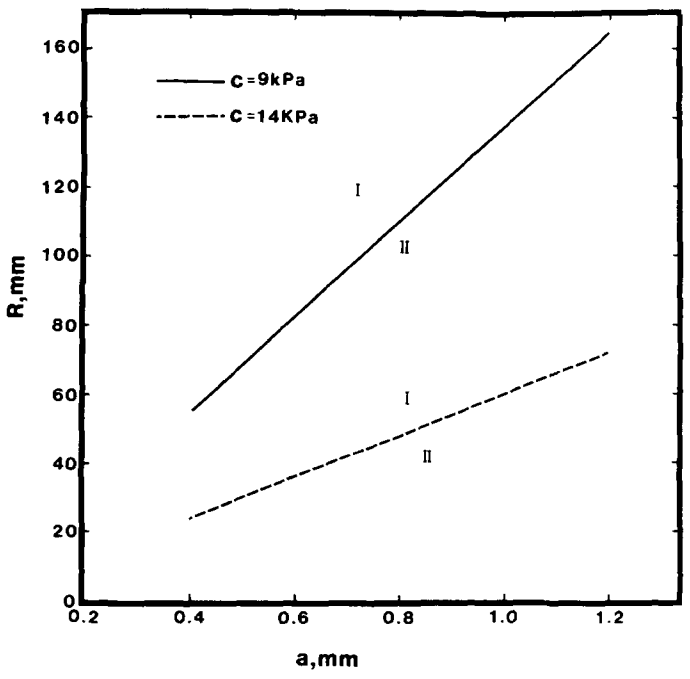

Fig. 7. Radius of the plastic front (R) as a function of the root radius (a). In region I, $R < b$ and in region II, $R > b$. The line dividing the regions I and II passes through the values of R for which $R = b$.

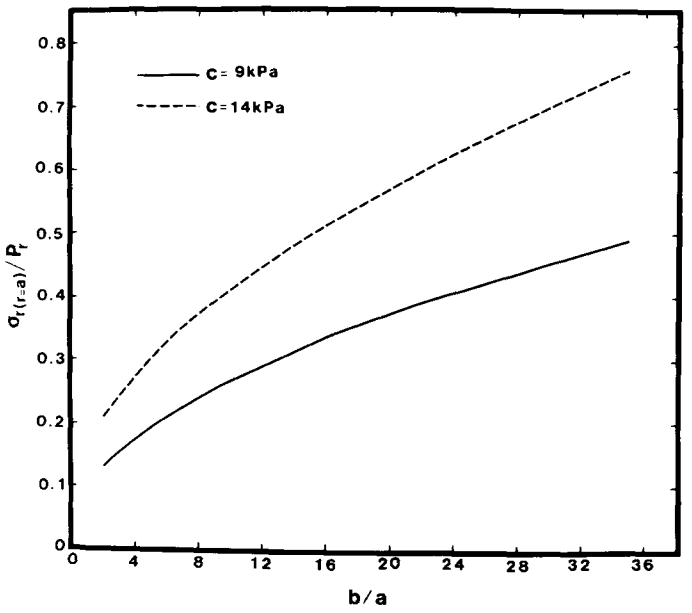

Fig. 8. The ratio of the radial stress adjacent to the root ($\sigma_{r(r=a)}$) and the maximum axial root growth pressure (P_r) as a function of dimensionless aggregate radius (b/a).

The boundary condition at $r = b$, $\sigma_r = 0$ is still valid. Substituting r by b in Eqn. 39 gives

$$\sigma_{r(r=b)} = D(1 + \sin\phi) - c\cot\phi \tag{41}$$

from which

$$D = \frac{c\cot\phi}{1 + \sin\phi} \tag{42}$$

Using the value of the constant D radial and tangential stresses at radii in the range $a < r < b$ can be estimated as

$$\sigma_r = c\cot\phi\,(b/r)^{2\sin\phi/(1+\sin\phi)} - c\cot\phi \tag{43}$$

and

$$\sigma_t = \frac{c\cot\phi}{1 + \sin\phi}\,(1 - \sin\phi)(b/r)^{2\sin\phi/(1+\sin\phi)} - c\cot\phi \tag{44}$$

The assumption that pressure in the radial direction is equal to the pressure in the axial direction may be now checked for the aggregates which fail plastically. A plot of the ratio $\sigma_{r(r=a)}/P_r$ as a function of b/a and c is given in Fig. 8 for the aggregate radii in the range of 2–14 mm and root radii in the range of 0.4–1.0 mm. R was re-evaluated from this plot and was found to be close to b. This shows that the radial pressure at $r = a$ has to be small to produce separate zones of plastic and elastic strain. In compressible soils[20], reasonable levels of radial pressure are

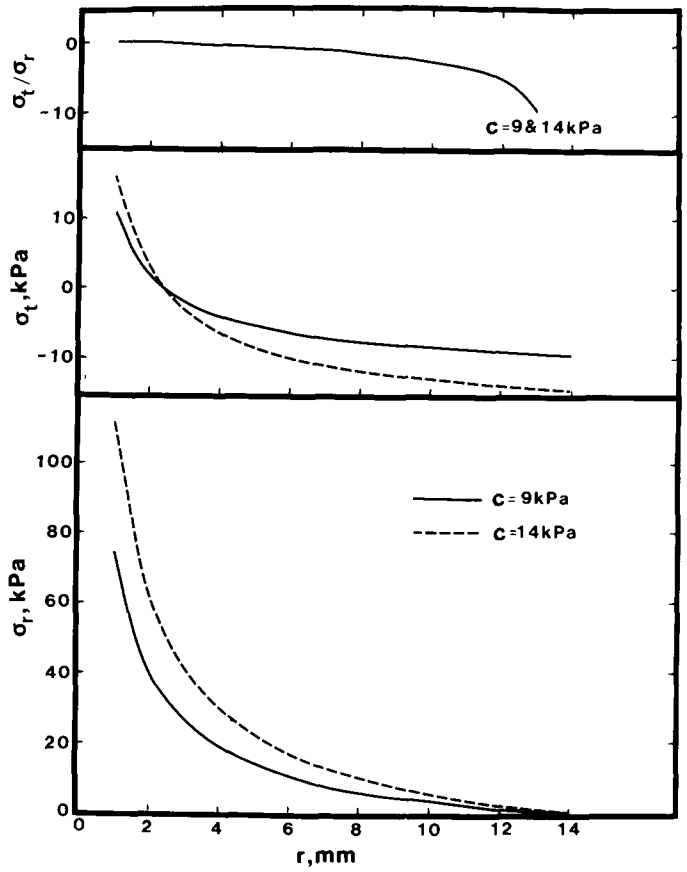

Fig. 9. Radial stress (σ_r), tangential stress (σ_t), and dimensionless stress ratio (σ_t/σ_r) as a function of the radial distance, r for aggregates of 14 mm radius and two different strengths.

involved in compressing soil in the radial direction during axial root growth. Therefore, $\sigma_{r(r=a)}$ is not a negligible amount of pressure. As seen from Fig. 8, for $\sigma_{r(r=a)}/P_r = 0.5$, strong aggregates ($c = 14$ kPa) of $b/a > 15$ would still be fully plastic. Hence, the assumption that $\sigma_{r(r=a)} = P_r$ is adequate since only plastic straining occurs in soil aggregates during root penetration.

The stresses σ_r and σ_t were estimated using Eqns 43 and 44 for an aggregate of 14 mm radius. Eqns 43 and 44 have no dependence on either root radius, a or the axial root growth pressure, P_r. Typical values of σ_r, σ_t and σ_t/σ_r as a function of radial distance, r, are given in Fig. 9. Both σ_r and σ_t decrease with increasing distance from the centre of the aggregate. Increasing the aggregate strength with c varying from

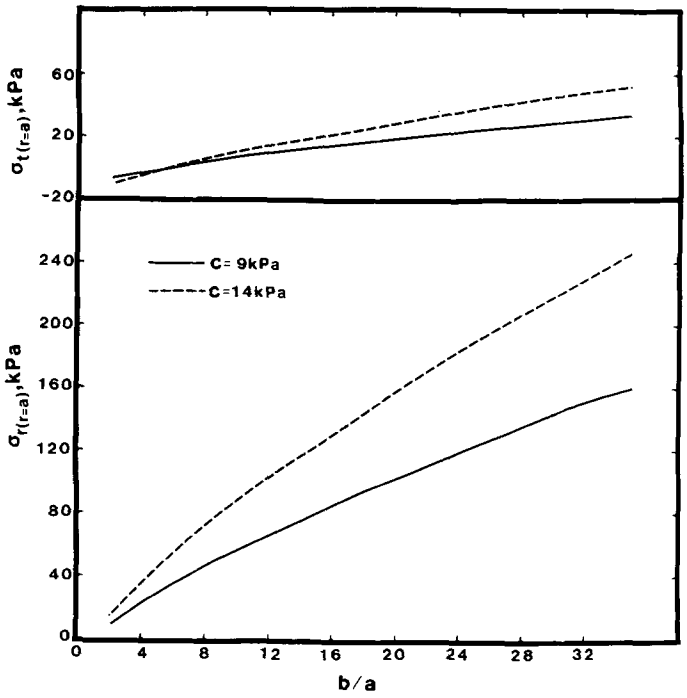

Fig. 10. Radial and tangential stresses adjacent to the root axis, $\sigma_{r(r=a)}$ and $\sigma_{t(r=a)}$, respectively, as a function of dimensionless aggregate radius (b/a).

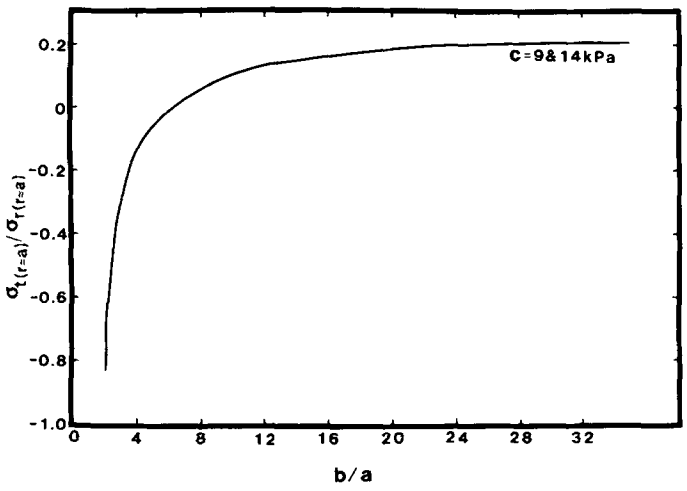

Fig. 11. Dimensionless stress ratio, $\sigma_{t(r=a)}/\sigma_{r(r=a)}$ adjacent to the root axis as a function of dimensionless aggregate radius (b/a).

9 to 14 kPa, the tangential stress decreases. For $r > b/2$, the ratio σ_t/σ_r decreased sharply indicating large increase in tensile stress relative to radial compressive stress.

The radial and tangential stresses adjacent to the root ($r = a$) were estimated with appropriate substitutions in Eqns 43 and 44, and they are plotted in Fig. 10 as functions of b/a. The radial stress, $\sigma_{r(r=a)}$ increased with increase in b/a and shear cohesion, c. The tangential stress, $\sigma_{t(r=a)}$ varied in a similar way except that the aggregates in the size range of $b < 5a$ were under tensile stress. Fig. 11 indicates that the dimensionless stress ratio, $\sigma_{t(r=a)}/\sigma_{r(r=a)}$ for all aggregates where $b > 20a$, remains constant. This is due to smaller changes in the tangential stress so that $\sigma_{t(r=a)}$ is only a small fraction of the radial stress for large aggregates. However, for smaller aggregates where $b < 10a$, the tensile stress increased sharply with decrease in aggregate size.

Comparison of root and probe stresses

The radial stress adjacent to the root, $\sigma_{r(r=a)}$, and the radial stress adjacent to the probe, P', can be compared for any value of b/a in Fig. 12. The ratio of these stresses, $\sigma_{r(r=a)}/P'$ was found to vary little in the range of 0.1–0.2 with change in b/a. The aggregate strength measured in terms of shear cohesion, c, also had a small effect on this ratio.

In Fig. 13, the ratio of the axial pressure exerted by the root to that exerted by a 1 mm diameter blunt probe, P_r/P' is given as a function of aggregate diameter. This ratio varied between 0.3 and 0.5 depending on the size and strength of aggregates. With the limited data obtained the ratio P_r/P' can be described by

$$P_r/P' = 0.7424 - 0.0228c - 0.0063\,d \quad (R^2 = 0.66) \quad (45)$$

where d (mm) is the aggregate diameter and c (kPa) is the shear cohesion of the aggregate.

Eqn 45 accommodates the slopes and intercepts of the two lines drawn for $c = 9$ kPa and $c = 14$ kPa in Fig. 13.

Discussion

The extent to which the size and strength of aggregates affected penetration by probes and roots was different (Figs. 5 and 6). This difference in behaviour cannot be attributed to the differences in root and probe diameters since the results are presented in terms of dimensionless aggregate radius, b/a. In our experiments, root diameters measured at the different points of the penetrating root axis

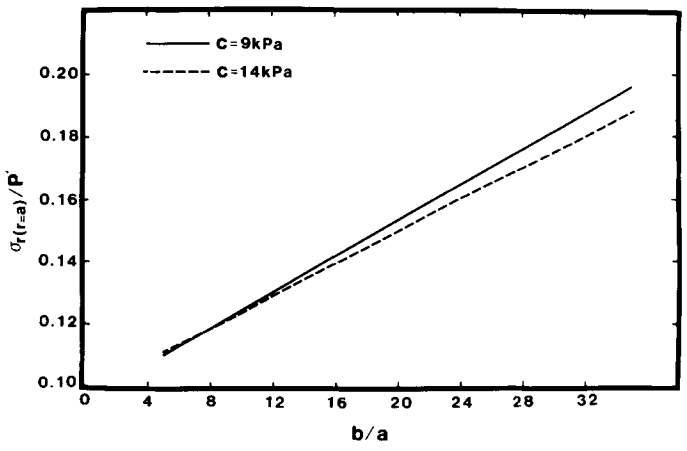

Fig. 12. The ratio of the predicted radial stress adjacent to the root axis ($\sigma_{r(r=a)}$) and experimental values of maximum (*axial*) penetrometer pressure (P') as a function of the dimensionless aggregate radius (b/a).

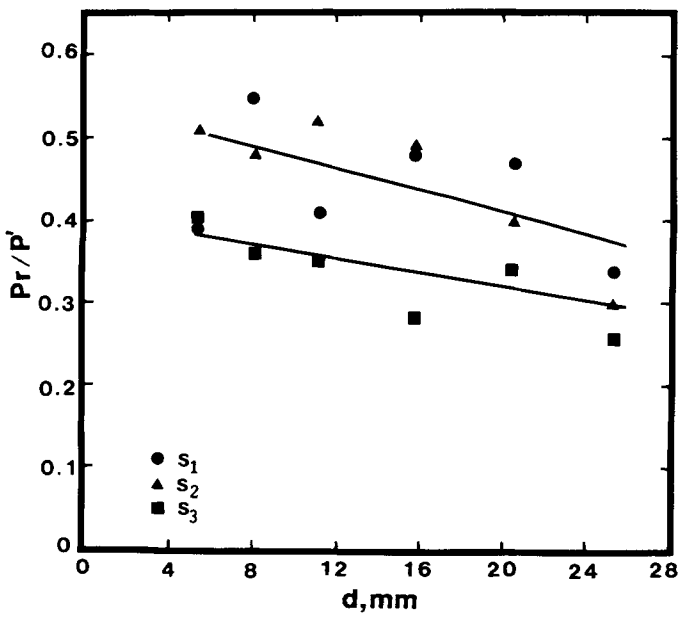

Fig. 13. Ratio of axial root growth pressure (P_r) to penetrometer pressure (P') as a function of aggregate diameter (d). The *top line* is the best fit for S_1 and S_2 aggregates (c = 9 kPa), and the *bottom line* is for S_3 aggregates (c = 13 kPa).

(RDT and RDA) were only slightly affected by aggregate size and strength (Tables 5 and 6). However, the diameter in the air gap (RDA) was much greater than that 1 mm behind the tip (RDT). This difference is attributed to increased mechanical impedance to root penetration. Root thickening in the air gap may be similar to thickening of the proximal end of the root, where the latter is known to influence root penetration[1,4,19].

The times, T_{max} for roots of the three plant species to reach the maximum force were significantly different (Table 3). When a plant root grows across an air gap (of zero strength) and meets a new surface, the wall pressure at the root surface increases by an additional quantity equal to the soil resistance[18]. The new increased wall pressure has to be counter-balanced by hydrostatic pressure for the root to continue penetration. As the root penetrates deeper into an aggregate, the soil resistance is increased. However, the soil resistance to root penetration increases only up to a finite depth until the aggregate fails due to increased tension. Aggregates of smaller size have less resistance to penetration (Figs. 3 and 5) and so the decrease in T_{max} with decrease in aggregate size (Fig. 4) may be due to two reasons. Firstly, small axial pressure is required to penetrate small aggregates and secondly, the root may reach the centre of the aggregate more quickly because of its small size.

The radial and tangential stresses adjacent to the root during penetration of aggregates of finite size (4–29 mm) are governed by plastic failure of the aggregate (Figs. 7 and 8). For any aggregate of finite size, the radial stress is maximum adjacent to the root and drops sharply with increasing distance r, from the axis (Fig. 9). Since the tensile stress increases rapidly with increased distance from the root, this stress may be considered responsible for causing aggregate failure during root penetration.

As aggregate size is increased, radial stress adjacenet to the probe is increased. Similarly, increased aggregate size (b/a) gives rise to increased radial stress adjacent to the root (Fig. 10). However, the development of tensile stress in aggregates during probe and root penetration is different both in magnitude and in the position in aggregate where it occurs. During probe penetration, maximum tensile stress occurs at the plastic front R, (Misra *et al.*)[25], whereas during root penetration, the tensile stress occurs adjacent to the root axis. The magnitude of tensile stress relative to the radial stress is higher during probe penetration than during root penetration.

It is evident from Figs. 12 and 13 that P_r/P' is much larger than $\sigma_{r(r=a)}/P'$. The difference arises because $\sigma_{r(r=a)}$ is a radial stress

predicted from c, ϕ, b and a, whereas P_r in Fig. 13 is the experimental axial root growth presssure expressed as a function of aggregate diameter, d. Both Figs. 12 and 13 emphasize that the resistance to root penetration is over-estimated by the probe. This may be due to the difference in the mode of soil deformation by the root and the probe, lower friction at the soil-root interface than at the soil-probe interface, root thickening at the proximal end and changes in the shape of the root tip[1,3,5,7,13,19,20,36,40].

Conclusions

The results of this study demonstrate the extent to which plant roots encounter mechanical stress when they penetrate aggregates of known size and strength. This has been achieved through a comparison of theoretical results for ideal, cylindrical aggregates with experimental results from approximately spherical aggregates. This comparison was necessary for theoretical and experimental feasibility. The errors involved in comparing these different shapes are probably negligible. The results can be applied to roots growing in macrostructured soil. It has been found that large axial root growth pressure must be exerted by roots to penetrate large aggregates. In any population of plants, only a small proportion of roots will be able to penetrate large aggregates. As a consequence, aggregate size will influence both plant growth and nutrient uptake.

Measurements of penetrometer pressure in the tilled layer are not very reliable, but a rough estimate of the soil resistance to root penetration can be obtained from a few simple measurements with the application of Eqn 45. The accuracy of this equation needs to be tested in future experiments using a wider range of soil cohesion values. A major assumption in part of this work was that the axial and radial root growth pressures were equal. Further experiments are needed to test this assumption.

Below the tilled layer, each aggregate is confined by the neighbouring aggregates. When plant roots penetrate confined aggregates, the mechanical stress to the root is increased by an additional amount. Under such circumstances, plant roots would have to exert greater axial growth pressure to penetrate confined aggregates than that is required for the unconfined aggregates in the tilled layer. The equation given by Whiteley *et al.*[40] to describe the effect of soil confinement on P'/P_r has to be modified to take into account the effects of the strength and size of aggregates.

References

1 Abdalla A M, Hettiaratchi D R P and Reece A R 1969 The mechanics of root growth in granular media. J. Agric. Engng. Res.14, 236–248.

2 Aubertin G M and Kardos L T 1965 Root growth through porous media under controlled conditions. I. Effect of pore size and rigidity. Soil Sci. Soc. Am. Proc. 29, 290–293.

3 Barley K P 1963 Influence of soil strength on growth of roots. Soil Sci. 96, 175–180.

4 Barley K P 1968 Deformation of the soil by the growth of plants. Trans. 9th Int. Congr. Soil Sci. Soc., Adelaide, pp 759–768.

5 Barley K P and Greacen E L 1967 Mechanical resistance as a soil factor influencing the growth of roots and underground shoots. Adv. Agron. 19, 1–43.

6 Barley K P, Farrell D A and Greacen E L 1965 The influence of soil strength on the penetration of a loam by plant roots. Aust. J. Soil Res. 3, 69–79.

7 Cockroft B, Barley K P and Greacen E L 1969 The penetration of clays by fine probes and root tips. Aust. J. Soil Res. 7, 333–348.

8 Dexter A R and Hewitt J S 1978 The deflection of plant roots. J. Agric. Engng. Res. 23, 17–22.

9 Dexter A R and Kroesbergen B 1985 Methodology for determination of tensile strength of soil aggregates. J. Agric. Engng. Res. 31, 139–147.

10 Dexter A R and Tanner D W 1972 Soil deformation induced by a moving cutting blade, an expanding tube and a penetrating sphere. J. Agric. Engng. Res. 17, 371–375.

11 Eavis B W and Payne D 1969 Soil physical conditions and root growth. *In* Root Growth. Ed W J Whittington, Butterworths, London, pp. 315–336.

12 Eavis B W, Ratliff L F and Taylor H M 1969 Use of a dead load technique to determine axial root growth pressure. Agron. J. 61, 640–643.

13 Farrell D A and Greacen E L 1966 Resistance to penetration of fine probes in compressible soil. Aust. J. Soil Res. 4, 1–17.

14 Gill W R and Bolt G H 1955 Pfeffer's studies of the root growth pressures exerted by plants. Agron. J. 47, 166–168.

15 Gill W R and Miller R D 1956 A method for study of the influence of mechanical impedance and aeration on the growth of seedling roots. Soil Sci. Soc. Am. Proc. 20, 154–157.

16 Gooderham P T 1973 Soil physical conditions and plant growth. Ph.D. Thesis, University of Reading.

17 Goss M J 1977 Effects of mechanical impedence on root growth in barley (*Hordeum vulgare* L.). I. Effects on the elongation and branching of seminal root axes. J. Exp. Bot. 28, 96–111.

18 Greacen E L and Oh J S 1972 Physics of root growth. Nature New Biol. 235, 24–25.

19 Greacen E L, Barley K P and Farrell D A 1969 The mechanics of root growth in soils with particular reference to the implications for root distribution. *In* Root Growth. Ed. W J Whittington, Butterworths, London, pp 256–269.

20 Greacen E L, Farrell D A and Cockroft B 1968 Soil resistance to metal probes and plant roots. Trans 9th Cong. Int. Soil Sci. Soc., Adelaide, pp 769–779.

21 Grimes D W, Miller R J and Wiley P L 1975 Cotton and corn root development in two field soils of different strength characteristics. Agron. J. 67, 519–523.

22 Johnson C M, Stout P R, Broyer T C and Carlton A B 1957 Comparative chlorine requirements of different plant species. Plant and Soil 8, 337–353.

23 Koolen A J and Kuipers H 1983 Agricultural soil mechanics. Springer Verlag, Heidelberg, Germany, 241 p.

24 Koolen A J and Vaandrager P 1984 Relationship between soil mechanical properties. J. Agric. Engng. Res. 29, 313–319.

25 Misra R K, Dexter A R and Alston A M 1985 Penetration of soil aggregates of finite size. I. Blunt penetrometer probes. Plant and Soil 94, 43–58.

26 Pfeffer W 1893 Druck und Arbeitsleistung durch Wachsende Pflanzen. Abhandlungen der Königlich Sächsischen Gesellschaft der Wissenschaften 33, 235–474.

27 Phillips R E and Kirkham D 1962 Mechanical impedance and corn seedling growth. Soil Sci. Soc. Am. Proc. 26, 319–322.
28 Stolzy L H and Barley K P 1968 Mechanical resistance encountered by roots entering compact soils. Soil Sci. 105, 297–301.
29 Taylor H M and Gardner H R 1960 Relative penetrating ability of different plant roots. Agron. J. 52, 579–581.
30 Taylor H M and Gardner H R 1963 Penetration of cotton seedling tap roots as influenced by bulk density, moisture content and strength of soil. Soil Sci. 96, 153–156.
31 Taylor H M and Ratliff L F 1969 Root growth pressures of cotton, peas and peanuts. Agron. J. 61, 398–402.
32 Taylor H M, Robertson G M and Parker J J Jr 1966 Soil strength-root penetration relations for medium to coarse textured soil materials. Soil Sci. 102, 18–22.
33 Timoshenko S and Goodier J N 1951 Theory of elasticity. McGraw-Hill Book Co. Inc., New York, USA, 506 p.
34 Veen B W 1982 The influence of mechanical impedance on the growth of maize roots. Plant and Soil 66, 101–109.
35 Vesić A S 1972 Expansion of cavities in infinite soil mass. J. Soil Mech. Fdn. Div., Proc. ASCE 98 (SM3), 265–290.
36 Voorhees W B, Farrell D A and Larson W E 1975 Soil strength and aeration effects on root elongation. Soil Sci. Soc. Am. Proc. 39, 948–953.
37 Whiteley G M and Dexter A R 1981 Elastic response of the roots of field crops. Physiol. Plant. 51, 407–417.
38 Whiteley G M and Dexter A R 1984 The behaviour of roots encountering cracks in soil. I. Experimental methods and results. Plant and Soil 77, 141–149.
39 Whiteley G M, Hewitt J S and Dexter A R 1982 The buckling of plant roots. Physiol. Plant. 54, 333–342.
40 Whiteley G M, Utomo W H and Dexter A R 1981 A comparison of penetrometer pressures and the pressures exerted by roots. Plant and Soil 61, 351–364.